Three-Dimensional FDTD Simulation of Electromagnetic Wave Transformation in a Dynamic Inhomogeneous Magnetized Plasma

Joo Hwa Lee, *Member, IEEE*, and Dikshitulu K. Kalluri, *Senior Member, IEEE*

Abstract— A three-dimensional (3-D) finite-difference time-domain (FDTD) algorithm is developed to study the transformation of an electromagnetic wave by a dynamic (time-varying) inhomogeneous magnetized plasma medium. The current density vector is positioned at the center of the Yee cube to accommodate the anisotropy of the plasma medium due to the presence of a static magnetic field. An appropriate time-stepping algorithm is used to obtain accurate solutions for arbitrary values of the collision frequency and the electron cyclotron frequency. The technique is illustrated by calculating the frequency shifts in a cavity due to a switched magnetoplasma medium with a time-varying and space-varying electron density profile.

Index Terms— Cavity, FDTD, time-varying magnetoplasma.

I. INTRODUCTION

FREQUENCY shifting of an electromagnetic wave in a time-varying plasma has been extensively studied [1]–[7] and some experiments [1]–[3] were carried out to demonstrate frequency shifting. Analytical studies make various assumptions and use simplified geometries including one-dimensional models, flash ionization, and slow or fast creation of the plasma medium [4]–[7].

A limited number of theoretical and numerical studies of three-dimensional (3-D) models are reported. Buchsbaum *et al.* [8] examined the perturbation theory for various mode configurations of a cylindrical cavity coaxial with a plasma column and coaxial with the static magnetic field. Gupta used a moment method to study cavities and waveguides containing anisotropic media and compared the results with the perturbation method [9]. A transmission-line-matrix (TLM) method was developed to study the interaction of an electromagnetic wave with a time-invariant and space-invariant magnetized plasma in 3-D space [10]. Mendonça [11] presented a mode-coupling theory in a cavity for a space-varying and slowly created isotropic plasma.

Since the introduction of the finite-difference time-domain (FDTD) method [12], it has been widely used in solving many electromagnetic problems including those concerned with plasma media [13], [14]. For the anisotropic cases [15], [16], the equations for the components of the current density vector become coupled and the implementation of the conventional FDTD scheme is difficult. We propose a new FDTD method to overcome this difficulty.

In this paper, we use the FDTD method to analyze the interaction of an electromagnetic wave with a magnetoplasma medium created in a cavity. This paper is organized as follows. The FDTD algorithm is derived first and the implementation of perfect electric conductor (PEC) boundary conditions is investigated. The algorithm is verified by using a mode-coupling theory and a perturbation technique. The application of the algorithm is illustrated by computing the new frequencies and amplitudes of the coupled modes generated due to a switched magnetized time-varying and space-varying plasma in a cavity with an initial TM mode excitation.

II. THREE-DIMENSIONAL FDTD ALGORITHM

A. Maxwell's Equation

Consider a time-varying magnetoplasma medium with collisions. Maxwell's equations and constitutive relation for a cold magnetoplasma are given by

$$\nabla \times \mathbf{E} = -\mu_0 \frac{\partial \mathbf{H}}{\partial t} \tag{1}$$

$$\nabla \times \mathbf{H} = \varepsilon_0 \frac{\partial \mathbf{E}}{\partial t} + \mathbf{J} \tag{2}$$

$$\frac{d\mathbf{J}}{dt} + \nu \mathbf{J} = \varepsilon_0 \omega_p^2(\mathbf{r}, t)\mathbf{E} + \boldsymbol{\omega}_b(\mathbf{r}, t) \times \mathbf{J} \tag{3}$$

where ε_0 is the permittivity of free-space, μ_0 the permeability of free-space, ω_p^2 the square of the plasma frequency, $\boldsymbol{\omega}_b = e\mathbf{B}_0/m_e$ the electron gyrofrequency, $\mathbf{B}_0$ the external static magnetic field, and e and m_e are the electric charge and mass of an electron, respectively. The field components in Cartesian coordinate are expressed as

$$\mathbf{E} = E_x \hat{x} + E_y \hat{y} + E_z \hat{z} \tag{4}$$

$$\mathbf{H} = H_x \hat{x} + H_y \hat{y} + H_z \hat{z} \tag{5}$$

$$\mathbf{J} = J_x \hat{x} + J_y \hat{y} + J_z \hat{z} \tag{6}$$

$$\boldsymbol{\omega}_b = \omega_{bx} \hat{x} + \omega_{by} \hat{y} + \omega_{bz} \hat{z}. \tag{7}$$

The substitutions of (4)–(7) in (1)–(3) give the following equations:

$$\frac{\partial H_x}{\partial t} = -\frac{1}{\mu_0}\left(\frac{\partial E_z}{\partial y} - \frac{\partial E_y}{\partial z}\right) \tag{8}$$

$$\frac{\partial E_x}{\partial t} = \frac{1}{\varepsilon_0}\left(\frac{\partial H_z}{\partial y} - \frac{\partial H_y}{\partial z} - J_x\right) \tag{9}$$

$$\begin{bmatrix} \dfrac{dJ_x}{dt} \\[4pt] \dfrac{dJ_y}{dt} \\[4pt] \dfrac{dJ_z}{dt} \end{bmatrix} = \mathbf{\Omega}\begin{bmatrix} J_x \\ J_y \\ J_z \end{bmatrix} + \varepsilon_0\omega_p^2(\mathbf{r},t)\begin{bmatrix} E_x \\ E_y \\ E_z \end{bmatrix} \tag{10}$$

where

$$\mathbf{\Omega} = \begin{bmatrix} -\nu & -\omega_{bz} & \omega_{by} \\ \omega_{bz} & -\nu & -\omega_{bx} \\ -\omega_{by} & \omega_{bx} & -\nu \end{bmatrix}. \tag{11}$$

The other components of $\mathbf{E}$ and $\mathbf{H}$ can be obtained in a similar manner.

B. FDTD Equations

Usual grid configuration for $\mathbf{J}$ is to place J_x, J_y, and J_z [17] at the locations of E_x, E_y, and E_z, respectively. This configuration works fine as long as the equations for the components of $\mathbf{J}$ are not coupled. When coupled as in (10), J_y and J_z are needed at the position of J_x to update J_x. However, the estimations of J_y and J_z at this position can be very complex; the maintenance of second-order accuracy requires averaging the values at four diagonal positions. Moreover, implementation of the averaging on the boundary is troublesome because some quantities outside the boundary are needed. We overcame these difficulties by placing $\mathbf{J}$ at the center of the Yee cube as shown in Fig. 1. The components of $\mathbf{J}$ are located at the same space point. It is now possible to solve (10) analytically since all variables are now available at the same space point. Treating $\mathbf{E}$, $\boldsymbol{\omega}_b$, ν, and
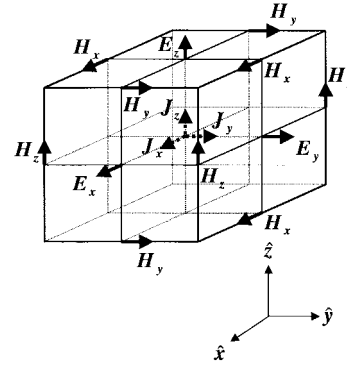

Fig. 1. Positioning of the electric, magnetic, and current density field vector components about a cubic unit cell.

ω_p as constants, each having an average value observed at the center of the time step, the Laplace transform of (10) leads to

$$\mathbf{J}(s) = (s\mathbf{I} - \mathbf{\Omega})^{-1}\mathbf{J}_0 + \varepsilon_0\omega_p^2\frac{1}{s}(s\mathbf{I} - \mathbf{\Omega})^{-1}\mathbf{E} \tag{12}$$

where $\mathbf{I}$ is the identity matrix. Inverse Laplace transform of (12) leads to the explicit expression for $\mathbf{J}(t)$ as

$$\mathbf{J}(t) = \mathbf{A}(t)\mathbf{J}_0 + \varepsilon_0\omega_p^2\mathbf{K}(t)\mathbf{E} \tag{13}$$

where as shown in (14)–(20) at the bottom of the page and $\omega_b^2 = \omega_{bx}^2 + \omega_{by}^2 + \omega_{bz}^2$. The FDTD equations for $\mathbf{J}$ are now expressed in terms of their values at a previous time step without having to solve simultaneous equations at each step

$$\begin{bmatrix} J_x|_{i,j,k}^{n+(1/2)} \\ J_y|_{i,j,k}^{n+(1/2)} \\ J_z|_{i,j,k}^{n+(1/2)} \end{bmatrix} = \mathbf{A}(\Delta t)\begin{bmatrix} J_x|_{i,j,k}^{n-(1/2)} \\ J_y|_{i,j,k}^{n-(1/2)} \\ J_z|_{i,j,k}^{n-(1/2)} \end{bmatrix} + \frac{\varepsilon_0}{2}\omega_p^2|_{i,j,k}^n\mathbf{K}(\Delta t)$$
$$\cdot\begin{bmatrix} E_x|_{i+(1/2),j,k}^n + E_x|_{i-(1/2),j,k}^n \\ E_y|_{i,j+(1/2),k}^n + E_y|_{i,j-(1/2),k}^n \\ E_z|_{i,j,k+(1/2)}^n + E_z|_{i,j,k-(1/2)}^n \end{bmatrix}. \tag{21}$$

In the above, the time step begins at $n - (1/2)$ and ends at $n + (1/2)$. This formulation is valid for arbitrary values of ν and $\boldsymbol{\omega}_b$; the idea is similar to the exponential time stepping [18]

$$\mathbf{A}(t) = \exp[\mathbf{\Omega}t]$$
$$= e^{-\nu t}\begin{bmatrix} C_1\omega_{bx}\omega_{bx} + \cos\omega_b t & C_1\omega_{bx}\omega_{by} - S_1\omega_{bz} & C_1\omega_{bx}\omega_{bz} + S_1\omega_{by} \\ C_1\omega_{by}\omega_{bx} + S_1\omega_{bz} & C_1\omega_{by}\omega_{by} + \cos\omega_b t & C_1\omega_{by}\omega_{bz} - S_1\omega_{bx} \\ C_1\omega_{bz}\omega_{bx} - S_1\omega_{by} & C_1\omega_{bz}\omega_{by} + S_1\omega_{bx} & C_1\omega_{bz}\omega_{bz} + \cos\omega_b t \end{bmatrix} \tag{14}$$

$$\mathbf{K}(t) = \mathbf{\Omega}^{-1}(\exp[\mathbf{\Omega}t] - \mathbf{I})$$
$$= \frac{e^{-\nu t}}{\omega_b^2 + \nu^2}\begin{bmatrix} C_2\omega_{bx}\omega_{bx} + C_3 & C_2\omega_{bx}\omega_{by} - C_4\omega_{bz} & C_2\omega_{bx}\omega_{bz} + C_4\omega_{by} \\ C_2\omega_{by}\omega_{bx} + C_4\omega_{bz} & C_2\omega_{by}\omega_{by} + C_3 & C_2\omega_{by}\omega_{bz} - C_4\omega_{bx} \\ C_2\omega_{bz}\omega_{bx} - C_4\omega_{by} & C_2\omega_{bz}\omega_{by} + C_4\omega_{bx} & C_2\omega_{bz}\omega_{bz} + C_3 \end{bmatrix} \tag{15}$$

$$S_1 = \sin\omega_b t/\omega_b \tag{16}$$

$$C_1 = (1 - \cos\omega_b t)/\omega_b^2 \tag{17}$$

$$C_2 = (e^{\nu t} - 1)/\nu - \nu C_1 - S_1 \tag{18}$$

$$C_3 = \nu(e^{\nu t} - \cos\omega_b t) + \omega_b\sin\omega_b t \tag{19}$$

$$C_4 = e^{\nu t} - \cos\omega_b t - \nu S_1 \tag{20}$$

for a high conductivity case. Also, if ν and ω_b are functions of time and space, (21) can be used by replacing those by $\nu|_{i,j,k}^n$ and $\omega_b|_{i,j,k}^n$ in (14)–(20).

Using the grid in Fig. 1, the following FDTD equations for the x components of $\mathbf{E}$ and $\mathbf{H}$ can be written

$$
\begin{aligned}
E_x|_{i+(1/2),\,j,\,k}^{n+1} & \\
= E_x|_{i+(1/2),\,j,\,k}^{n} & + \frac{1}{\varepsilon_0} \\
\cdot & \left[\frac{\Delta t}{\Delta y} \left(H_z|_{i+(1/2),\,j+(1/2),\,k}^{n+(1/2)} - H_z|_{i+(1/2),\,j-(1/2),\,k}^{n+(1/2)} \right) \right. \\
& \left. - \frac{\Delta t}{\Delta z} \left(H_y|_{i+(1/2),\,j,\,k+(1/2)}^{n+(1/2)} - H_y|_{i+(1/2),\,j,\,k-(1/2)}^{n+(1/2)} \right) \right] \\
& - \frac{\Delta t}{2\varepsilon_0} \left(J_x|_{i+1,\,j,\,k}^{n+(1/2)} + J_x|_{i,\,j,\,k}^{n+(1/2)} \right)
\end{aligned} \tag{22}
$$

$$
\begin{aligned}
H_x|_{i,\,j+(1/2),\,k+(1/2)}^{n+(1/2)} & \\
= H_x|_{i,\,j+(1/2),\,k+(1/2)}^{n-(1/2)} & - \frac{1}{\mu_0} \\
\cdot & \left[\frac{\Delta t}{\Delta y} \left(E_z|_{i,\,j+1,\,k+(1/2)}^{n} - E_z|_{i,\,j,\,k+(1/2)}^{n} \right) \right. \\
& \left. - \frac{\Delta t}{\Delta z} \left(E_y|_{i,\,j+(1/2),\,k+1}^{n} - E_y|_{i,\,j+(1/2),\,k}^{n} \right) \right].
\end{aligned} \tag{23}
$$

The other components can be written in a similar way.

The stability condition of this method is not easily expressed in a simple form due to the complexity of the algorithm. Nevertheless, it can be said that the standard stability criterion can be applied, i.e., the stability is governed by the mode whose phase velocity is fastest in the medium [19], [20].

C. PEC Boundary Conditions

Fig. 2 shows the locations of the fields on x–y plane. The indexes k and $k+(1/2)$ of the planes correspond to those in the FDTD equations. J_x, J_y, J_z, E_x, E_y, and H_z are located on k plane, whereas E_z, H_x, and H_y are located on $k+(1/2)$ plane. For a perfect conductor the tangential components of $\mathbf{E}$ field and the normal component of $\mathbf{H}$ field vanish on the boundaries. Hence, it is natural to choose PEC boundaries to correspond to a k rather than a $k+(1/2)$ plane. For example, the plane $k=1$ may be used for the bottom PEC of a cavity. The boundary conditions are satisfied by assigning zero value to E_x, E_y, J_x, J_y, and H_z on $k=1$ plane. Since J_z is not zero on the $k=1$ plane, we need to update its value with time. From (21), the values $E_z|_{i,j,(3/2)}^n$ and $E_z|_{i,j,(1/2)}^n$ are needed to obtain the updated value $J_z|_{i,j,1}^{n+(1/2)}$. We note that the PEC boundary condition $\partial E_n/\partial n = 0$ will permit us to modify (21) for $k=1$ as given in the following:

$$
\begin{aligned}
\begin{bmatrix} J_x|_{i,j,1}^{n+(1/2)} \\ J_y|_{i,j,1}^{n+(1/2)} \\ J_z|_{i,j,1}^{n+(1/2)} \end{bmatrix} = & \mathbf{A}(\Delta t) \begin{bmatrix} J_x|_{i,j,1}^{n-(1/2)} \\ J_y|_{i,j,1}^{n-(1/2)} \\ J_z|_{i,j,1}^{n-(1/2)} \end{bmatrix} + \frac{\varepsilon_0}{2} \omega_P^2|_{i,j,1}^n \mathbf{K}(\Delta t) \\
& \cdot \begin{bmatrix} E_x|_{i+(1/2),j,1}^n + E_x|_{i-(1/2),j,1}^n \\ E_y|_{i,j+(1/2),1}^n + E_y|_{i,j-(1/2),1}^n \\ 2E_z|_{i,j,(3/2)}^n \end{bmatrix}.
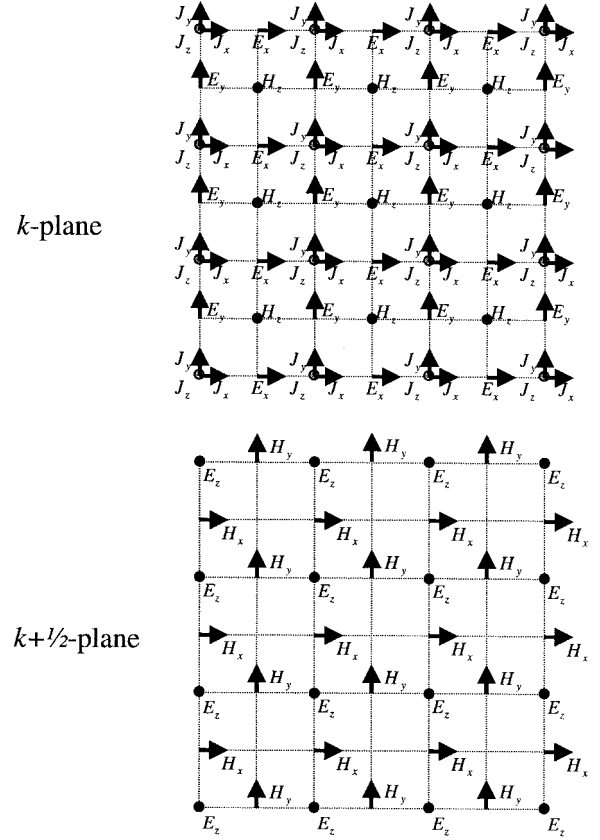\end{aligned} \tag{24}
$$

Fig. 2. Construction of planes for a simple implementation of the PEC boundary conditions.

The algorithm given above leads to explicit computation while maintaining second-order accuracy.

III. VALIDATION OF THE ALGORITHM

The algorithm is validated by considering two test cases for which results are obtained by other techniques. The first test case involves switching of a plasma medium in a rectangular microwave cavity with dimensions L_x, L_y, and L_z. Several cavity modes are excited due to the interaction of the incident mode and the plasma medium. Hence, the new fields may be written in terms of cavity modes as

$$
\mathbf{E}(\mathbf{r}, t) = \sum a_l(t) \mathbf{E}_l(\mathbf{r}) \tag{25}
$$

where $\mathbf{E}_l(\mathbf{r})$ is a normalized cavity mode and

$$
\int \mathbf{E}_l(\mathbf{r}) \mathbf{E}_{l'}^*(\mathbf{r}) d^3 r = \delta_{ll'}. \tag{26}
$$

In the above, $\mathbf{E}^*$ is the complex conjugate of $\mathbf{E}$. For the space-varying but isotropic plasma creation, the differential equations for a are obtained by the mode coupling theory as [11]

$$
\frac{\partial^2 a_l(t)}{\partial t^2} + \omega_l^2 a_l + \sum C_{ll'} a_{l'} = 0 \tag{27}
$$

where

$$\omega_l^2 = c^2 k^2$$
$$= c^2 \left[\left(\frac{m\pi}{L_x} \right)^2 + \left(\frac{p\pi}{L_y} \right)^2 + \left(\frac{q\pi}{L_z} \right)^2 \right] \quad (28)$$

$$C_{ll'} = \int \omega_p^2(\mathbf{r}, t) \mathbf{E}_l(\mathbf{r}) \mathbf{E}_{l'}^*(\mathbf{r}) d^3 r \quad (29)$$

and m, p, q are the mode numbers.

Consider the creation of a time-varying and space-varying plasma medium in the cavity with a plasma frequency profile $\omega_p^2(\mathbf{r}, t)$

$$\omega_p^2(\mathbf{r}, t) = \omega_{p0}^2 \left(1 - e^{-t/T_r} \right) \exp \left[-\left(\alpha_x \frac{x - x_0}{L_x} \right)^2 \right.$$
$$\left. - \left(\alpha_y \frac{y - y_0}{L_y} \right)^2 - \left(\alpha_z \frac{z - z_0}{L_x} \right)^2 \right]$$
$$t > 0 \quad (30)$$

where ω_{p0}^2 is the saturation plasma frequency, T_r is a rise time, and the spatial variation is Gaussian. If the spatial variation of the plasma is only in x direction, i.e., $\alpha_y = \alpha_z = 0$, newly excited modes should have same mode numbers for p and q. Therefore, we need to consider the changes in mode number m only to describe the fields in the cavity.

Fig. 3 shows the comparisons of the results by FDTD with those by the mode coupling theory for the initial TM_{111} mode excitation. Isotropic and inhomogeneous plasma distribution is considered for comparisons. The following parameters are used: $L_x = 4L_y = 4L_z$, $T_r = 0$, $x_0 = L_x/2$, $\omega_{p0} = \omega_0$, $\nu = 0$, $\alpha_x = 1$, $\alpha_y = \alpha_z = 0$, and ω_0 is the frequency of the initial mode. The results for the mode-coupling theory are obtained by numerically solving the differential equations (27) with the initial conditions obtained from the initial excitation. The results for the FDTD are obtained first by calculating $\mathbf{E}(\mathbf{r}, n\Delta t)$ using our algorithm and then by computing $a_l(t)$

$$a_l(t) = a_l(n\Delta t) = \int \mathbf{E}(\mathbf{r}, n\Delta t) \mathbf{E}_l^*(\mathbf{r}) d^3 r. \quad (31)$$

Fig. 3 shows very good agreement.

The second validation is for the case of a magnetized plasma. Results based on a perturbation method are available for a magnetized low-density plasma filled cavity in [21]. In the perturbation theory, the frequency shift due to homogeneous magnetized plasma can be obtained as

$$\frac{\Delta\omega}{\omega_0} \approx -\frac{1}{2} \int \varepsilon_0 \mathbf{E}(\mathbf{r}) \Delta\varepsilon \mathbf{E}^*(\mathbf{r}) d^3 r \quad (32)$$

where $\Delta\varepsilon = \varepsilon - \mathbf{I}$ and ε is the dielectric tensor of the magnetized plasma medium. For the magnetized plasma problem, a differential equation similar to (27) is not available. Nevertheless, the new fields can be approximated by (25) and the empty cavity modes can be used to extract the modes from FDTD simulation for a weak plasma density since the coupling is not strong. During the FDTD computations, $a_l(t)$ is computed using (31) and the frequency change is obtained
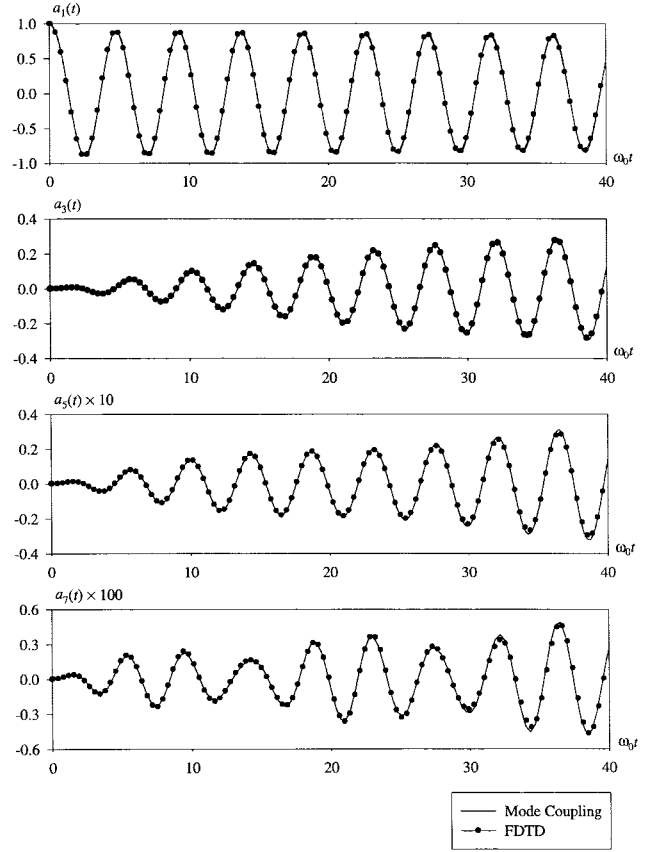

Fig. 3. Mode amplitudes for the case of a switched isotropic plasma in a cavity. Comparisons of the FDTD and the mode-coupling theory are shown. The coefficients are normalized with respect to $a_1(0)$. $a_m(t)$ indicates $a_{m11}(t)$.
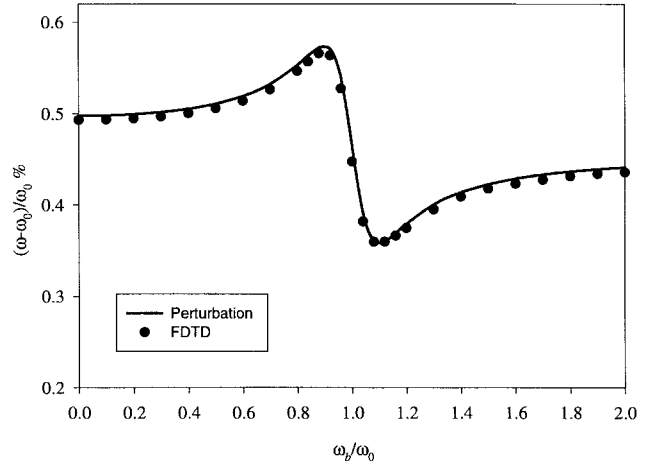

Fig. 4. Frequency shift due to creation of a low-density homogeneous magnetized plasma in a cavity. Comparisons of the FDTD and the perturbation methods. The ratio of frequency shift (%) versus the cyclotron frequency ω_b/ω_0 is plotted. $\omega_p/\omega_0 = 0.1$ and $\nu/\omega_0 = 0.1$.

from the time series of $a_l(t)$ by Prony method [22]. Fig. 4 shows the comparison of the perturbation and FDTD methods for an initial TM_{111} mode excitation. A lossy ($\nu/\omega_0 = 0.1$) homogeneous plasma medium ($\omega_p/\omega_0 = 0.1$) is used and the dimensions of the cavity are given by $9L_x = 4L_y = 3L_z$. The background magnetic field $\boldsymbol{\omega}_b(\mathbf{r}) = \omega_b \hat{z}$ is along z axis. Since we have computed the final frequency shift which is
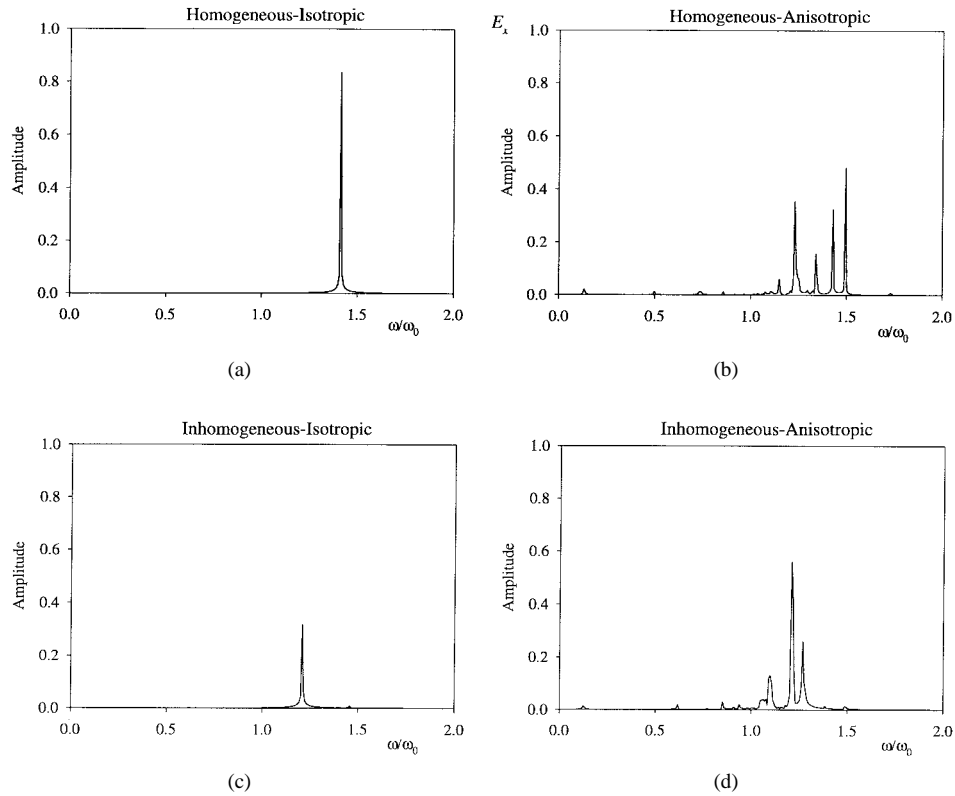
Fig. 5. Amplitude spectra of the electric field E_x at $x = (1/15)L_x$, $y = (7/15)L_y$, $z = (7/15)L_z$. Parameters are $T_r = 100/\omega_0$, $\omega_{p0} = \omega_0$, $\nu = 0$. (a) Homogeneous-isotropic ($\alpha_x = \alpha_y = \alpha_z = 0$, $\boldsymbol{\omega}_b = 0$). (b) Homogeneous-Anisotropic ($\alpha_x = \alpha_y = \alpha_z = 0$, $\boldsymbol{\omega}_b = \omega_0\hat{z}$). (c) Inhomogeneous-isotropic ($\alpha_x = \alpha_y = \alpha_z = 2$, $\boldsymbol{\omega}_b = 0$). (d) Inhomogeneous-anisotropic ($\alpha_x = \alpha_y = \alpha_z = 2$, $\boldsymbol{\omega}_b = \omega_0\hat{z}$).

independent of the rise time T_r, we have considered the case of sudden ($T_r = 0$) creation. In this figure, the frequency shift ratio is depicted for various background magnetic field intensities.

IV. ILLUSTRATIVE EXAMPLES OF THE NEW FDTD METHOD FOR A DYNAMIC MEDIUM

Fig. 5 shows the frequency shifting due to the interaction of the electromagnetic wave with a time-varying and space-varying magnetized plasma. A rectangular cavity with an initial excitation of TM_{111} mode is considered with following parameters: $6L_x = 3L_y = 2L_z$, $T_r = 100/\omega_0$, $x_0 = L_x/2$, $y_0 = L_y/2$, $z_0 = L_z/2$, $\omega_{p0} = \omega_0$, and $\nu = 0$. $\alpha_x = \alpha_y = \alpha_z = 0$ is used for homogeneous plasma distribution [Fig. 5(a) and (b)] and $\alpha_x = \alpha_y = \alpha_z = 2$ is used for inhomogeneous plasma distribution [Fig. 5(c) and (d)]. The electron cyclotron frequency $\boldsymbol{\omega}_b$ is chosen to be zero for Fig. 5(a) and (c), and $\boldsymbol{\omega}_b = \omega_0\hat{z}$ for (b) and (d). The results are obtained from the spectrum of the time series of E_x at $x = (1/15)L_x$, $y = (7/15)L_y$, $z = (7/15)L_z$ taken after the plasma is almost fully created, i.e., after $t = 6.4T_r$. For a homogeneous and isotropic creation of plasma [Fig. 5(a)] the frequency shift due to the interaction of the electromagnetic wave with the plasma is the same as that of an unbounded plasma. For the cavity with an anisotropic uniform plasma [Fig. 5(b)] several new modes appear. It is noted that some of the modes have higher frequencies than that of the unbounded isotropic plasma. A comparison of Fig. 5(a) with (c) and Fig. 5(b) with (d) shows

that nonuniformly filled plasma cavity displays lower values of frequency shifts for the same maximum values of ω_{p0} as predicted in [11].

V. CONCLUSION

Three-dimensional FDTD formulations are constructed for time-varying inhomogeneous magnetoplasma medium. An explicit formulation is accomplished by locating $\mathbf{J}$ at the center of the Yee cube and by using an appropriate time stepping algorithm.

REFERENCES

[1] E. Yablonovitch, "Spectral broadening in the light transmitted through a rapidly growing plasma," *Phys. Rev. Lett.*, vol. 31, pp. 877–879, 1973.

[2] C. J. Joshi, C. E. Clayton, K. Marsh, D. B. Hopkins, A. Sessler, and D. Whittum, "Demonstration of the frequency upshifting of microwave radiation by rapid plasma creation," *IEEE Trans. Plasma Sci.*, vol. 18, pp. 814–818, Oct. 1990.

[3] S. P. Kuo and J. Faith, "Interaction of an electromagnetic wave with a rapidly created spatially periodic plasma," *Phys. Rev. E*, vol. 56, no. 2, pp. 1–8, 1997.

[4] D. K. Kalluri, V. R. Goteti, and A. M. Sessler, "WKB solution for wave propagation in a time-varying magnetoplasma medium: Longitudinal propagation," *IEEE Trans. Plasma Sci.*, vol. 21, no. 1, pp. 70–76, Feb. 1993.

[5] J. H. Lee and D. K. Kalluri, "Modification of an electromagnetic wave by a time-varying switched magnetoplasma medium: Transverse propagation," *IEEE Trans. Plasma Sci.*, vol. 26, no. 1, pp. 1–6, Feb. 1998.

[6] D. K. Kalluri and T. T. Huang, "Longitudinal propagation in a magnetized time-varying plasma: Development of Green's function," *IEEE Trans. Plasma Sci.*, vol. 26, no. 3, pp. 1022–1030, June 1998.

[7] D. K. Kalluri, *Electromagnetics of Complex Media.* Boca Raton: CRC, 1998.

[8] S. J. Buchsbaum, L. Mower, and S. C. Brown, "Interaction between cold plasmas and guided electromagnetic waves," *Phys. Fluids*, vol. 3, no. 5, pp. 806–819, 1960.

[9] R. R. Gupta, "A study of cavities and waveguides containing anisotropic media," Ph.D. dissertation, Syracuse University, Syracuse, NY, July 1965.

[10] T. Kashiwa, N. Yoshida, and I. Fukai, "Transient analysis of a magnetized plasma in three-dimensional space," *IEEE Trans. Antennas Propagat.*, vol. 36, pp. 1096–1105, Aug. 1988.

[11] J. T. Mendonça and L. Oliveira e Silva, "Mode coupling theory of flash ionization in a cavity," *IEEE Trans. Plasma Sci.*, vol. 24, no. 1, pp. 147–151, Feb. 1996.

[12] K. S. Yee, "Numerical solution of initial boundary value problems involving Maxwell's equations in isotropic media," *IEEE Trans. Antennas Propagat.*, vol. AP-14, pp. 302–307, May 1966.

[13] J. L. Young, "A full finite difference time domain implementation for radio wave propagation in a plasma," *Radio Sci.*, vol. 29, pp. 1513–1522, 1994.

[14] S. A. Cummer, "An analysis of new and existing FDTD methods for isotropic cold plasma and a method for improving their accuracy," *IEEE Trans. Antennas Propagat.*, vol. 45, pp. 392–400, Mar. 1997.

[15] S. G. García, T. M. Hung-Bao, R. G. Martín, and B. García Olmedo, "On the application of finite methods in time domain to anisotropic dielectric waveguides," *IEEE Trans. Microwave Theory*, vol. 44, pp. 2195–2205, Dec. 1996.

[16] J. Schneider and S. Hudson, "The finite-difference time-domain method applied to anisotropic material," *IEEE Trans. Antennas Propagat.*, vol. 41, pp. 994–999, July 1993.

[17] E. Sano and T. Shibata, "Fullwave analysis of picosecond photoconductive switches," *IEEE J. Quantum Electron.*, vol. 26, no. 2, pp. 372–377, Feb. 1990.

[18] A. Taflove, *Computational Electrodynamics: The Finite-Difference Time-Domain Method.* Boston, MA: Artech House, 1995.

[19] A. Taflove and M. E. Brodwin, "Numerical solution of steady-state electromagnetic scattering problems using the time-dependent Maxwell's equations," *IEEE Trans. Microwave Theory Tech.*, vol. MTT-23, no. 8, pp. 623–630, Aug. 1975.

[20] J. L. Young and F. P. Brueckner, "A time domain numerical model of a warm plasma," *Radio Sci.*, vol. 29, no. 2, pp. 451–463, 1994.

[21] R. F. Harrington, *Field Computation by Moment Methods.* Malabar, FL: Krieger, 1968.

[22] N. Kannan and D. Kundu, "On modified EVLP and ML methods for estimating superimposed exponential signals," *Signal Processing,* vol. 39, pp. 223–233, 1994.

Joo Hwa Lee (SM'97,'98–M'99) was born in Seoul, Korea. He received the B.S. degree in physics from the Seoul National University, Seoul, Korea, in 1986, and the M.S. and Ph.D. degrees in physics from the University of Massachusetts, Lowell, in 1994 and 1998, respectively.

From 1986 to 1991, he worked for Samsung Data Display as an Engineer for cathode ray tube research including electromagnetic analysis and optical systems design. He is now a Research Associate at the Electromagnetics and Complex Media Research Laboratory, University of Massachusetts, Lowell. His interests include electromagnetic wave interactions with time-varying plasma medium, using FDTD algorithm. He is also interested in channel simulation in communication systems.

Dikshitulu K. Kalluri (M'60–M'84–SM'89) was born in Chodavaram, India. received the B.E. degree in electrical engineering from Andhra University, Waltair, India, the D.I.I. Sc. degree in high-voltage engineering from the Indian Institute of Science, Bangalore, India, the M.S. degree in electrical engineering from the University of Wisconsin, Madison, and the Ph.D. in electrical engineering from the University of Lawrence, KS, in 1968.

He is currently a Professor of electrical and computer engineering at the University of Massachusetts, Lowell. He began his career at the Birla Institute of Technology, Ranchi, India, advancing to the rank of Professor and heading the Electrical Engineering Department, serving as (Dean) Assistant Director of the Institute. He has collaborated with research groups at the Lawrence Berkeley Laboratory, University of California, Los Angeles, the University of Southern California, Los Angeles, and the University of Tennessee, Knoxville, and has worked several summers as a faculty Research Associate at Air Force Laboratories, Hanscom. Since 1984 he has been with the University of Massachusetts, Lowell, where he is Coordinator of the doctoral program and Codirector of the Center for Electromagnetic Materials and Optical Systems (CEMOS). As a part of the center, he recently established the Electromagnetics and Complex Media Research Laboratory. He is the author of *Electromagnetics of Complex Media* (Boca Raton, FL: CRC, 1998).

Dr. Kalluri is a Fellow of the Institute of Electronic and Telecommunication Engineers and a member of Eta Kappa Nu and Sigma Xi.